Slow Motional ESR in Complex Fluids: The Slowly Relaxing Local Structure Model of Solvent Cage Effects

Antonino Polimeno[†] and Jack H. Freed*

Baker Laboratory of Chemistry, Cornell University, Ithaca, New York 14853-1301

Received: February 17, 1995; In Final Form: May 3, 1995[⊗]

A detailed formulation is presented for the analysis of slow motional ESR in terms of the reorientation of the probe molecule within a dynamic solvent cage. This formulation is appropriate for isotropic and ordered fluids. The solvent cage is modeled in terms of a set of collective variables that represent the instantaneous solvent structure around the probe and that reorient on a slower time scale than the probe. This "slowly relaxing local structure" model is incorporated into an augmented stochastic Liouville equation that is solved by efficient computational means which enables nonlinear least squares fitting to experimental spectra. This formulation is applied to some recent slow motional ESR spectra obtained at 250 GHz. Such high-frequency ESR spectra have been shown to be particularly sensitive to the microscopic details of the molecular reorientational process. Significant improvements are found in fitting the ESR spectra for the cases studied, viz., perdeuterated 2,2,6,6-tetramethyl-4-piperidone (PDT) in toluene and 3-doxylcholestane (CSL) in *o*-terphenyl (OTP), a glass-forming liquid, when compared to a model of simple Brownian reorientation. In both cases the cage is found to relax at least 1 order of magnitude slower than the probe itself, and it provides a potential for probe reorientation on the order of $2-7\ k_BT$. The cage potential for the PDT case is characterized by minima at more than one orientational angle, allowing for jump-type reorientations between such minima superimposed on substantial local motions suggestive of earlier simulations based on a simple jump model. For CSL in OTP, weak negative ordering is found, consistent with an oblate-shaped local structure provided by the OTP solvent molecules. These examples illustrate the potential of utilizing high-frequency slow motional ESR to discern details of solvent interactions associated with molecular reorientations in fluids.

1. Introduction

With the advent of very high field ESR requiring resonant radiation at wavelengths on the order of $\lambda = 1-2$ mm, corresponding to frequencies above 140 GHz, the rotational dynamics of spin-labeled molecules observed by ESR is more commonly found to be in the slow motional regime than is the case at conventional ESR frequencies (e.g. 9.5 GHz).[1-4] This slow motional regime corresponds to the limit $\tau_R\Delta\omega \geq 1$, where τ_R is the correlation time for the rotational dynamics and $\Delta\omega$ is a measure of the magnitude of the orientation-dependent part of the spin Hamiltonian. For this regime, the spectral line shapes take on a complex form which is found to be sensitive to the microscopic details of the motional process. This is to be contrasted with the fast motional regime, for which $\tau_R\Delta\omega \ll 1$, where simple Lorentzian line shapes are obtained, and only estimates of τ_R (or more precisely a rotational diffusion tensor) may be obtained independent of the microscopic details of the molecular dynamics. Note that it is the enhanced role of the g tensor that results in the significantly greater $\Delta\omega$ for 250 GHz.

Another important feature of the very high field ESR spectrum in the slow motional regime (as well as in the rigid limit) is the enhanced orientational selectivity, which is largely due to the greatly enhanced g tensor resolution. In this regime, regions of the spectrum corresponding to the magnetic x, y, and z molecular axes are clearly discerned, and this provides improved sensitivity to the details of the microscopic features for the rotational diffusion.[1-4]

The interpretation of these slow motional spectra requires an analysis based upon sophisticated theory, and it is usually carried out by means of the stochastic Liouville equation (SLE), which can be solved numerically to obtain the ESR spectrum that is predicted for various Markovian models of reorientation.[5,6] In the past, partly for the sake of computational convenience, simple Markovian models have been employed that merely distinguish between reorientations by large, moderate, or small (i.e. Brownian) jump diffusion.[1-6] While these models proved to be useful, they beg the issue of the details of the interaction of the probe molecule with the solvent molecules and in so doing may be regarded as oversimplified and idealized models. Solvent interaction and participation is generally regarded as important, as for example has been amply demonstrated in earlier ESR studies in a wide variety of fluids.[7-12] These have included viscous liquids, glass-forming liquids, liquid crystals, and highly polar liquids.

The main drawback of including solvent coordinates in even an approximate fashion is the increased number of degrees of freedom that must be considered explicitly, and this can lead to unwieldy computational challenges. We have recently been engaged in significant efforts to develop improved but tractable stochastic models to describe rotational motions in liquids.[13-15] The many-body problem of dealing with the microscopic details of the (complex) fluid is replaced by a set of collective degrees of freedom that approximately represent the main effects of the complex medium in the immediate surroundings of the rotating solute. Following this approach, we have formalized the commonly held intuitive model of a loose solvent "cage" in terms of a set of collective variables that represent the instantaneous structure of the solvent molecules around the reorienting probe. This loose "cage" is thereby considered as a dynamical structure relaxing in the same or slower time range as does the solute and may thus be regarded as a "slowly relaxing local structure" (SRLS) model, of the type which has

[†] On leave of absence from Department of Physical Chemistry, University of Padova, Italy.

[⊗] Abstract published in *Advance ACS Abstracts,* June 15, 1995.

0022-3654/95/2099-10995$09.00/0

previously been utilized in very simple form to discuss ESR spectra.[7-9,12,16-18] What results is an effective two-body model for which, in the simplest case, a two-body Smoluchowski equation is obtained. It formally represents the rotational diffusion of two interacting rigid rotors and thereby increases the number of degrees of freedom by the three Euler angles for the orientation of the cage. The formulation and rigorous solution of this model and a host of related but more sophisticated models have now been detailed.[13-15] This work supersedes the earlier simplified treatments[7-9,12,16,18] which could not be utilized for slow motional ESR spectra.

This recent work provides the basis whereby the rotational dynamics may be represented by multidimensional Markov processes (e.g. coupled Smoluchowski equations). In the present work we focus on the inclusion of such multidimensional Markov processes into the stochastic Liouville equation and the methods of their solution. We shall see that the "symmetry-breaking" features of the spin Hamiltonian (which has cylindrical symmetry in the lab frame), as opposed to the isotropic symmetry of the SRLS model (in a macroscopically isotropic fluid), lead to a significantly more complicated SLE. Nevertheless, despite the increased degrees of freedom and complexity, previously developed algorithms[6,19-21] enable us to efficiently compute the predicted ESR spectra.

The utility of the SRLS model for fitting slow motional ESR spectra in liquids is illustrated in this work with some recent examples from this laboratory of slow motional spectra obtained at 250 GHz (corresponding to $\lambda = 1.22$ mm and $B_0 = 8.9$ T). These examples include the slow rotational diffusion of two probes: PDT (2,2,6,6-tetramethyl-4-piperidone), which is a relatively small and nearly spherical probe, in toluene and CSL (3-doxylcholestane), a larger, cigar-shaped molecule, in a glass-forming liquid, OTP (*o*-terphenyl). As a result of the computational efficiency of our algorithms, it was possible to utilize nonlinear least squares fitting of the theory to the experimental spectra. In the context of the SRLS model we are able to obtain rather detailed pictures of the solvent cage structure and dynamics for these examples.

In section 2 we outline the stochastic Liouville approach for including the SRLS model in the slow motional ESR analysis. In section 3 the basic features of the SRLS model are described and the resulting augmented SLE is presented. The details of obtaining a satisfactory matrix representation of this SLE and its efficient solution are given in section 4. In section 5, we present the analysis of recent experiments utilizing the SRLS model. A summary appears in section 6.

2. The Stochastic Liouville Approach

We start with the SLE for the CW-ESR spectrum of a spin probe in a condensed fluid.[1,6] We characterize the orientation and position of the probe by the coordinates $\mathbf{Q}^\circ = (\mathbf{r}^\circ,\mathbf{\Omega}^\circ)$, i.e. the position of the center of mass and the Euler angles specifying the orientation of the probe with respect to an inertial frame of reference, hereafter called the laboratory frame (LF). The probe spin Hamiltonian describing the magnetic interactions is taken as[5,6]

$$\hat{\mathscr{H}} = (\beta_e/\hbar)\mathbf{B}_0\cdot\mathbf{g}\cdot\hat{\mathbf{S}} + \gamma_e\hat{\mathbf{I}}\cdot\mathbf{A}\cdot\hat{\mathbf{S}} \qquad (1)$$

where β_e is the Bohr magneton, $\hbar$ is the Planck constant, γ_e is the electron gyromagnetic ratio, and the Hamiltonian is expressed in angular frequency units. The first term is the electronic Zeeman interaction with the magnetic field $\mathbf{B}_0$; the second term describes the hyperfine interaction between the nuclear spin operator $\hat{\mathbf{I}}$ and the electron spin operator $\hat{\mathbf{S}}$. Other interaction terms (e.g. spin-rotational coupling and nuclear Zeeman) will be neglected for simplicity, although their introduction does not affect our treatment. The definition of each tensor and tensor operator in the proper frame of reference will be given in the following section. Both the **g** and **A** tensors will depend upon the probe coordinates $\mathbf{Q}^\circ$.

According to the stochastic Liouville approach, the density matrix operator $\sigma(\mathbf{Q}^\circ,t)$ describing the joint evolution of the quantum spin degrees of freedom and the classical motion coordinates $\mathbf{Q}^\circ$ is described by the semiclassical equation

$$(\partial/\partial t)\hat{\sigma}(\mathbf{Q}^\circ,t) = -(\hat{\Gamma} + i\hat{\mathscr{H}}^\times)\hat{\sigma}(\mathbf{Q}^\circ,t) \qquad (2)$$

where $\hat{\mathscr{H}}^\times$ is the quantum Liouville operator, i.e. the commutator superoperator defined with respect to $\hat{\mathscr{H}}$, while $\hat{\Gamma}$ is Markovian (e.g. a Smoluchowski or Fokker–Planck) operator describing the stochastic drift of the probe position and orientation in the condensed phase. The quantity $\hat{\Gamma} + i\hat{\mathscr{H}}^\times$ is referred to as the stochastic Liouville superoperator. The magnetic resonance spectrum for an unsaturated, frequency-swept CW-ESR experiment is then given in compact notation as[5,6]

$$I(\omega) = \frac{1}{\pi}\mathscr{R}\langle v|[(\hat{\Gamma} + i\hat{\mathscr{H}}^\times) + i(\omega - \omega_0)\hat{1}]^{-1}|v\rangle \qquad (3)$$

where ω is the sweep frequency, $\omega_0 = g_0\beta_eB_0/\hbar = \gamma_eB_0$, with $g_0 = (1/3)(g_{xx} + g_{yy} + g_{zz})$. The starting vector $|v\rangle$, with respect to which the resolvent is evaluated, is in part a unit vector of the allowed ESR transitions in Liouville space, and thus it is actually an operator in Hilbert space acting on the spin degrees of freedom. It is also a function of the probe coordinates $\mathbf{Q}^\circ$ (see below). The symbol $\mathscr{R}$ in eq 3 implies the real part of the expression to its right.

Typically in the past, only the probe orientation and/or its position in space has been included in the stochastic description, as pointed out above. This is equivalent to a Brownian-like assumption that the rest of the fluid in the condensed phase produces random forces and torques with a white noise spectrum. In real fluids this is certainly not true. In order to account for the collective modes arising from the local behavior of solvent molecules in the immediate neighborhood of the probe, it is sensible to adopt an augmented Fokker–Planck (FP) or Smoluchowski (S) operator $\hat{\Gamma}(\mathbf{Q}^\circ,\mathbf{Q}^c)$ which describes static and dynamic solvent effects in the form of additional degrees of freedom $\mathbf{Q}^c$ coupled to the probe ones $\mathbf{Q}^\circ$.[14-17] The SLE of eq 2 or 3 is then modified accordingly by using an augmented FP or S operator $\hat{\Gamma}(\mathbf{Q}^\circ,\mathbf{Q}^c)$ instead of a simple jump-type or Brownian one, $\hat{\Gamma}(\mathbf{Q}^\circ)$. We also replace $\sigma(\mathbf{Q}^\circ,t) \rightarrow \sigma(\mathbf{Q}^\circ,\mathbf{Q}^c,t)$ in eqs 2 and 3.

From the several cases of augmented FP or S equations analyzed by Polimeno and Freed[14] we shall employ the simplest model for describing the rotational behavior of the probe in the presence of a SRLS. The model[13,14] assumes $\mathbf{Q}^\circ = \mathbf{\Omega}^\circ$ and $\mathbf{Q}^c = \mathbf{\Omega}^c$; that is, the relevant stochastic degrees of freedom are given by the Euler angles specifying the orientation of the probe *and* of SRLS. This neglect of positional coordinates in the SRLS appears to be justified by recent molecular dynamics simulations of cage effects in a simple fluid,[15] but would not be adequate for a structured fluid such as a smectic liquid crystal.[22-24]

3. Augmented Stochastic Liouville Equation

We shall describe the coupled system of probe + SRLS in terms of a series of frames of reference, which are illustrated in Figure 1. First, the laboratory frame (LF), which is an inertial reference frame, is taken as a frame at rest whose z axis is parallel to the applied magnetic field $\mathbf{B}_0$. Next we consider a

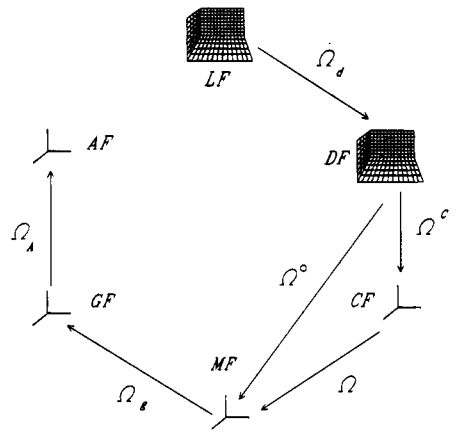

Figure 1. Reference frames which define the structural and dynamic properties of the combined system of spin-bearing probe molecule and solvent cage: LF = lab frame, DF = director frame, MF = molecular frame, CF = cage frame, GF = g tensor frame, AF = A tensor frame.

second inertial frame, the director frame (DF), fixed with respect to the LF, which is relevant only for ordered phases in which there is a macroscopic direction of alignment or director (e.g. nematic or smectic liquid crystals). The probe is reorienting with respect to the LF (or alternatively the DF), and its orientation is specified by the instantaneous orientation of the molecular frame (MF). The MF will be taken as defined by the principal axes of the rotational diffusion tensor of the probe. As is usual,[5,6,9,11,24] it will be assumed for simplicity that the principal axes of alignment of the probe in an ordered phase will coincide with this MF. The local structure or cage is also reorienting with respect to the LF (or the DF), and its instantaneous orientation is specified by the cage frame (CF) taken as the principal axes of its rotational diffusion tensor as well as its principal axes of alignment in an oriented phase. Finally we consider the magnetic frames of reference for the molecular g and A tensors (GF and AF), which are fixed with respect to the MF. The Euler angles specifying the transformation of vectors and tensors from one system to the other are summarized in the following scheme, where the notation $F_1 \rightarrow F_2(\Omega_{12})$ means that if by $\mathbf{E}_{12} = \mathbf{E}(\Omega_{12})$ we identify the Euler matrix[25] whose elements are calculated from the Euler angles Ω_{12}, then a vector whose components in the frame F_2 are given by $\mathbf{v}_2$ will be given in the frame F_1 by $\mathbf{v}_1 = \mathbf{E}_{12}\mathbf{v}_2$:

$$\left.\begin{array}{l} \mathrm{LF} \xrightarrow{\Omega_d} \mathrm{DF} \\ \mathrm{DF} \xrightarrow{\Omega^c} \mathrm{CF} \\ \mathrm{DF} \xrightarrow{\Omega^\circ} \mathrm{MF} \\ \mathrm{MF} \xrightarrow{\Omega_g} \mathrm{GF} \\ \mathrm{GF} \xrightarrow{\Omega_A} \mathrm{AF} \end{array}\right\} \quad (4)$$

Notice that in this scheme Ω_d, Ω_g, and Ω_a are constant angles, since they specify relative orientations between mutually fixed frames, whereas Ω^c and Ω° are time-dependent stochastic quantities.

We may now completely define the augmented stochastic Liouville operator in the following form:

$$\hat{\mathscr{L}} = \hat{\Gamma}(\Omega^\circ,\Omega^c) + i\hat{\mathscr{H}}^\times \quad (5)$$

where $\hat{\Gamma}(\Omega^\circ,\Omega^c)$ is a two-body Smoluchowski operator to be specified, and $\hat{\mathscr{H}}^\times$ is the quantum Liouville operator briefly defined in the previous section. Let us now first consider the precise definition of the spin Liouville part.

Following a notation introduced by Freed and co-workers,[5,6] we write the spin Liouvillian as the zero-rank tensor which results from the contraction of zero and second-rank irreducible spherical tensors or tensor operators:

$$\begin{aligned} \hat{\mathscr{H}}^\times &= \sum_{\mu=g,A}\sum_{l=0,2}\sum_{m=-l}^{l} F_{\mu,L}^{(l,m)*}\,\hat{A}_{\mu,L}^{(l,m)} \\ &= \sum_{\mu=g,A}\sum_{l=0,2}\sum_{m=-l}^{l}\sum_{m'=-l}^{l}\sum_{m''=-l}^{l} \times \\ &\qquad \mathscr{D}^l_{mm'}(\Omega_d)\mathscr{D}^l_{m'm''}(\Omega^\circ)F_{\mu,M}^{(l,m'')*}\hat{A}_{\mu,L}^{(l,m)} \end{aligned} \quad (6)$$

where $X_{\mu,N}^{(l,m)}$ stands for the mth component ($m = -l, \ldots, l$) in the N frame of the lth ($l = 0, 2$) rank irreducible spherical tensor or tensor operator, X, which relates to the interaction μ ($\mu = g$ or A); $\mathscr{D}^l_{mk}(\Omega)$ is a generic Wigner rotation matrix in Ω (we adopt the Rose convention[6,26]). The molecular components of the F tensors are defined in terms of their components in the proper magnetic frame:

$$F_{g,M}^{(l,m)*} = \sum_{m'=-l}^{l} \mathscr{D}^l_{mm'}(\Omega_g)F_{g,G}^{(l,m')*} \quad (7)$$

$$F_{A,M}^{(l,m)*} = \sum_{m'=-l}^{l}\sum_{m''=-l}^{l} \mathscr{D}^l_{mm'}(\Omega_g)\mathscr{D}^l_{m'm''}(\Omega_A)F_{A,A}^{(l,m'')*} \quad (8)$$

The components of the F and A tensor operators[5,6,11] are summarized in Appendix A. Note that the Liouville operator does not depend in any way upon the solvent or cage degrees of freedom. Indeed, the magnetic interactions terms, which do depend upon the absolute orientation of the molecule (cf. eq 6) are strictly an internal property of the probe molecule.

The dynamical coupling between probe and collective solvent modes is contained in the two-body Smoluchowski operator:[14,17]

$$\hat{\Gamma} = \hat{\mathbf{J}}^\circ\cdot\mathbf{R}^\circ\cdot P_{eq}\hat{\mathbf{J}}^\circ P_{eq}^{-1} + \hat{\mathbf{J}}^c\cdot\mathbf{R}^c\cdot P_{eq}\hat{\mathbf{J}}^c P_{eq}^{-1} \quad (9)$$

Here $\hat{\mathbf{J}}^\circ$ is equal to the vector operator that generates an infinitesimal rotation of the probe (but for a factor $-i$), with components specified in the MF; $\hat{\mathbf{J}}^\circ$ is the equivalent operator for the cage, with components specified in the CF. The diffusional tensors $\mathbf{R}^\circ$ and $\mathbf{R}^c$ are time-independent and diagonal in the MF and in the CF, respectively, as described above. The Boltzmann distribution P_{eq} is defined with respect to a generic potential $V(\Omega^\circ,\Omega^c)$:

$$P_{eq}(\Omega^\circ,\Omega^c) = \exp[-V(\Omega^\circ,\Omega^c)/k_BT]/\langle\exp[-V(\Omega^\circ,\Omega^c)/k_BT]\rangle \quad (10)$$

and

$$V(\Omega^\circ,\Omega^c) = V^\circ(\Omega^\circ) + V^{int}(\Omega^\circ - \Omega^c) + V^c(\Omega^c) \quad (11)$$

Equation 11 includes mean field terms $V^\circ(\Omega^\circ)$ and $V^c(\Omega^c)$ representing the respective alignment of the probe and of the cage in an ordered phase. The most important term for the SRLS model is the interaction potential $V^{int}(\Omega^\circ - \Omega^c)$ between the probe and the cage, which depends upon their relative orientation, $\Omega = \Omega^\circ - \Omega^c$. (Note that $\Omega_{21} \equiv \Omega_2 + \Omega_1$ stands for the Euler angles representing the rotation obtained by first applying rotation 1 (Ω_1) and then rotation 2 (Ω_2)). The angular brackets in eq 10 imply an ensemble average.

It is customary and convenient to expand the potential in terms of the Wigner rotation matrices $\mathscr{D}^l_{mk}(\Omega)$, which represent a complete orthogonal set for expanding an arbitrary function $f(\Omega)$. In the case of $V^\circ(\Omega^\circ)$ for an ordered phase this

sum may be restricted by the following symmetries.[5,6,24] (1) In a uniaxial phase (e.g. nematic or smectic A) the potential must be cylindrically symmetric about the director. That is, letting $\mathbf{\Omega}^\circ = (\alpha^\circ,\beta^\circ,\gamma^\circ)$, the potential must be independent of the angle α°, restricting m to $m = 0$. (2) Inversion symmetry of the potential restricts l to even values (note $\mathscr{D}^l_{0k}(\mathbf{\Omega}^\circ)^* \propto Y^l_k(\beta^\circ,\gamma^\circ)$, the spherical harmonic of rank l and order k). (3) Since $V^\circ(\mathbf{\Omega}^\circ)$ is real, then the expansion coefficients (cf. eq 12 below) must obey $a^l_k = (-)^k(a^l_{-k})^*$. Also, for $V^\circ(\mathbf{\Omega}^\circ)$ to have a relatively simple dependence upon $\mathbf{\Omega}^\circ$, one should restrict its expansion to the lowest even l values, since spherical harmonics of increasing l will have an increasing number of nodes. Typically one lets $l = 2$ or 4. Also, we note that the a^2_k ($k = -2, ..., 2$) are the five components of a second-rank irreducible tensor, for which in their principal axis system (in which the associated Cartesian second-rank tensor components are diagonal) only a^2_0 and $(a^2_2 + a^2_{-2})$ are nonzero. We will also assume for simplicity, as is usually done, that only a^4_0, $(a^4_2 + a^4_{-2})$, and $(a^4_4 + a^4_{-4})$ are nonzero in this axis system, which is equivalent to invoking D_2 point group molecular symmetry for $V^\circ(\mathbf{\Omega}^\circ)$. Thus we shall write

$$v^\circ(\mathbf{\Omega}^\circ) \equiv \frac{1}{k_B T} V(\mathbf{\Omega}^\circ) = -\sum_{l=2,4} \{a^l_0 \mathscr{D}^l_{00}(\mathbf{\Omega}^\circ) + a^l_2[\mathscr{D}^l_{02}(\mathbf{\Omega}^\circ) + \mathscr{D}^l_{0-2}(\mathbf{\Omega}^\circ)]\} \quad (12)$$

ignoring the terms with $k = 4$ for simplicity. We shall assume, partially for convenience, a very similar form for $V^c(\mathbf{\Omega}^c)$:

$$v^c(\mathbf{\Omega}^c) \equiv \frac{1}{k_B T} V(\mathbf{\Omega}^c) = -\sum_{l=2,4} \{b^l_0 \mathscr{D}^l_{00}(\mathbf{\Omega}^c) + b^l_2[\mathscr{D}^l_{02}(\mathbf{\Omega}^c) + \mathscr{D}^l_{0-2}(\mathbf{\Omega}^c)]\} \quad (13)$$

In dealing with the interaction potential $V^{int}(\mathbf{\Omega})$ it is tempting to utilize an analogous functional form:

$$v^{int}(\mathbf{\Omega}) \equiv \frac{1}{k_B T} V^{int}(\mathbf{\Omega}) = -\sum_{l=2,4} \{c^l_0 \mathscr{D}^l_{00}(\mathbf{\Omega}) + c^l_2[\mathscr{D}^l_{02}(\mathbf{\Omega}) + \mathscr{D}^l_{0-2}(\mathbf{\Omega})]\} \quad (14)$$

However, it is probably oversimplified to regard the instantaneous local orienting potential of the probe with respect to the cage as necessarily obeying the macroscopic symmetry constraints of typical ordered phases. Thus, it is not unreasonable to expect that the local cage can have a biaxial character,[15] such that terms in $\mathscr{D}^l_{mk}(\mathbf{\Omega})$ with $m \neq 0$ can appear in eq 14. Similarly, we might expect that the summation in eq 14 need not be restricted to even l terms. For this latter matter, it is useful to first note that the anisotropic interaction terms in the spin Hamiltonian of eq 6 have $l = 2$. Then we note that second-rank correlation functions are qualitatively very similar whether a first- or a second-rank SRLS potential is used.[14] One may expect such a feature to persist in the slow motional regime. Thus, for economy in fitting parameters, and for convenience, we will restrict l to just even values. In the same spirit we shall ignore in the present work any biaxial terms with $m \neq 0$ in eq 14. [Note, however, a variation on eq 14 whereby biaxiality can be introduced without a large additional number of parameters to fit. That is, we assume eq 14 applies but for an $\mathbf{\Omega}' \equiv \mathbf{\Omega}^\circ - \mathbf{\Omega}^{c'}$ where c' denotes a cage frame that is tilted relative to the CF defined above as the principal axes of rotation and of alignment of the cage. Then we may replace the $\mathscr{D}^l_{0k}(\mathbf{\Omega})$ in eq 14 by

$$\mathscr{D}^l_{0k}(\mathbf{\Omega}') = \sum_n \mathscr{D}^l_{0n}(-\mathbf{\Omega}^r)\mathscr{D}^l_{nk}(\mathbf{\Omega}) \quad (15)$$

where $\mathbf{\Omega}^r$ specifies the Euler angles for the rotation of the CF into the tilted cage frame specified by c', i.e. $\mathbf{\Omega}^r \equiv -\mathbf{\Omega}^{c'} + \mathbf{\Omega}^c$. If it is possible to let $\mathbf{\Omega}^r = (0,\beta^r,0)$, i.e. by a single tilt angle, then this would not very substantially increase the fitting parameters.]

An additional feature that we are neglecting for simplicity is a distribution in the magnitude of $v^{int}(\mathbf{\Omega})$ and its possible fluctuations. Such features do appear in the molecular dynamics simulations for a simple fluid.[15]

We have now completely defined the model. The orientational and dynamical behavior of the probe is defined by the dimensionless coefficients of expansion of the mean field potential a^l_k ($l = 2, 4$; $k = 0, 2$) and by its rotational diffusion tensor $\mathbf{R}^\circ$; the cage is described by the expansion coefficients of the mean field potential b^l_k ($l = 2, 4$; $k = 0, 2$) and by its rotational diffusion tensor, $\mathbf{R}^c$. The mutual interaction is measured by the coefficients in the expansion of the interaction potential c^l_k ($l = 2, 4$; $k = 0, 2$).

[It is of interest to compare the present augmented SLE with one that was utilized by Liang et al.[34] to deal with additional degrees of freedom (ADF) in the case of micellar structures. Unlike our model in which the motions of probe and cage are coupled through the $v^{int}(\mathbf{\Omega})$ of eq 14, their ADF were assumed to be statistically independent of the probe dynamics. Their ADF included the overall tumbling of the micelle and the translational diffusion of the labeled molecule (probe) around the surface of the micelle. Such effects were introduced by an additional transformation in eq 6 to include, for example, the orientation of the micelle itself. In such a model, the probe moves in the moving frame of the micelle's orientation, and the statistical independence of both motions implies there is no slip of the probe; that is, it exactly follows the slow orientations of the micelle. In our model, developed for local solvent structure, the ADF can be easily decoupled from the probe motion merely by letting $v^{int}(\mathbf{\Omega}) \rightarrow 0$, whereas the limit of no slip is achieved by letting $v^{int}(\mathbf{\Omega}) \rightarrow \infty$.]

4. Computational Treatment

We shall proceed to evaluate numerically eq 3 by expanding the augmented stochastic Liouville operator of eq 5 in matrix form in the direct product space spanned by a complete orthonormal set of functions in $\mathbf{\Omega}^\circ$ and in $\mathbf{\Omega}^c$ and a set of electron and nuclear spin "projection operators". The resulting matrix/vector formulation will then be solved numerically by employing the Lanczos algorithm, which has been shown to be a powerful tool for the efficient diagonalization of large sparse complex symmetric matrices.[19-21] The procedure which is followed is best described by Schneider and Freed,[6] and its application to many-body stochastic operators is described by Polimeno and Freed.[14]

4.1. Basis Sets. The main challenge in planning an efficient strategy for the numerical solution of eq 3, which involves complicated algebra in calculating the matrix elements, is a sensible choice for the set of basis functions used in the expansion. Also, in order to minimize the number of functions required to achieve a reasonable convergence in the evaluation of the spectrum, the inherent symmetries have to be fully utilized. One alternative could be to define a nonorthogonal basis set[20] which relates to the equilibrium distribution of the system probe + cage. In practice, this kind of choice leads to major complications in computing the spin Liouville part of the operator. Also, one could employ angular momentum coupling techniques, as was done for isotropic fluids by Polimeno and Freed.[14] Unfortunately, their usefulness is much reduced by the presence of the spin Liouville operator (which

is a function of Ω°, and *not* of Ω) and by the mean field terms in the potential, $V^\circ(\Omega^\circ)$ and $V^c(\Omega^c)$. All things considered, we found that the best strategy was to generate a direct product basis set, $|\Sigma\rangle\rangle$ in which probe and cage are described by 10 distinguishable quantum numbers. That is

$$|\Sigma\rangle\rangle = |L^\circ M^\circ K^\circ L^c M^c K^c p^S q^S p^I q^I\rangle\rangle = |L^\circ M^\circ K^\circ\rangle \otimes |L^c M^c K^c\rangle \otimes |p^S q^S p^I q^I\rangle\rangle \quad (16)$$

with

$$|L^\circ M^\circ K^\circ\rangle = \sqrt{\frac{[L^\circ]}{8\pi^2}}\mathscr{D}^{L^\circ}_{M^\circ K^\circ}{}^*(\Omega^\circ) \quad (17)$$

$$|L^c M^c K^c\rangle = \sqrt{\frac{[L^c]}{8\pi^2}}\mathscr{D}^{L^c}_{M^c K^c}{}^*(\Omega^c) \quad (18)$$

and the standard Liouville spin basis sets,

$$|\sigma\rangle\rangle = |p^S q^S p^I q^I\rangle\rangle = (|S,m_S\rangle\langle S,m'_S|) \otimes (|I,m_I\rangle\langle I,m'_I|) \quad (19)$$

are used. The double angular brackets in these expressions imply ket vectors in Liouville space. Note in eqs 17 and 18 $[L] = 2L + 1$. Thus, the basis set is built as a direct product of normalized Wigner functions for the probe and for the cage. Note that the normalized Wigner functions (eqs 17 and 18) are eigenfunctions of the quantum Hamiltonian of a symmetric top.[25,26] The spin basis functions are a direct product of projectors for the electron spin (quantum numbers S and m_S) and the nuclear spin (quantum numbers I and m_I). It is convenient[6,11] to define the spin quantum numbers $p^S \equiv m_S - m'_S$, $q^S \equiv m_S + m'_S$, $p^I \equiv m_I - m'_I$, and $q^I \equiv m_I + m'_I$.

In order to simplify somewhat the treatment below, we shall assume that the cage mean field potential of eq 13 is cylindrically symmetric so that only the coefficients b^l_0, $l = 2$ and 4, are nonzero, i.e. $b^l_k = 0$, $k \neq 0$. We shall also use the interaction potential of eq 14, which, when expanded in terms of Ω° and Ω^c as shown below, is also cylindrically symmetric with respect to the cage variables. Thus, whereas the cage quantum number for $L^c \neq 0$ couples into the ESR spectrum via $V^{int}(\Omega)$ in eq 5, the quantum number $K^c = 0$. Thus even for an axially symmetric cage rotational diffusional tensor, for which

$$\hat{\mathbf{J}}^c\cdot\mathbf{R}^c\cdot\hat{\mathbf{J}}^c|L^c M^c K^c\rangle = [R^c_\perp L^c(L^c+1) + (R^c_\parallel - R^c_\perp)(K^c)^2]|L^c M^c K^c\rangle \quad (20)$$

only the $R^c_\perp$ will enter into the needed expressions. For convenience we shall let $R^c_\perp \equiv R^c$). Since these conditions yield $K^c = 0$, we will ignore K^c below. The basis set defined by eq 16 thus contains nine *relevant* quantum numbers in the following range:

$$\left.\begin{array}{ll} L^\circ: & 0 \le L^\circ_{max} \\ M^\circ: & -L^\circ \le M^\circ \le L^\circ \\ K^\circ: & -L^\circ \le K^\circ \le L^\circ \\ L^c: & 0 \le L^c_{max} \\ M^c: & -L^c \le M^c \le L^c \\ p^S: & -1 \le p^S \le 1 \\ q^S: & -1 + |p^S|, 1 - |p^S| \\ p^I: & -2I \le p^I \le 2I \\ q^I: & -2I + |p^I|, -2I + |p^I| + 2, ..., 2I - |p^I| \end{array}\right\} \quad (21)$$

where we have set the spin quantum number of the electron $S = 1/2$. L°_{max} and L^c_{max} represent the maximum values of these quantum numbers in the finite basis set expansion (cf. section 4.3).

Given the structure of the terms in eq 5, it will be useful to symmetrize the basis set with respect to K°.[5,6] Thus, following Meirovitch et al.,[11]

$$|p^S q^S p^I q^I; L^\circ M^\circ K^\circ j^K L^c M^c\rangle\rangle_K = \mathscr{N}^K[|L^\circ M^\circ K^\circ L^c M^c K^c p^S q^S p^I q^I\rangle\rangle + j^K s^K |L^\circ M^\circ - K^\circ L^c M^c K^c p^S q^S p^I q^I\rangle\rangle] \quad (22)$$

where

$$s^K = (-)^{L^\circ + K^\circ} \quad (23)$$

$$\mathscr{N}^K = [2(1 + \delta_{K^\circ,0})]^{-1/2} \quad (24)$$

and now K° is a non-negative number. Also, when $K^\circ = 0$, $j^K = (-)^{L^\circ}$, and for $0 < K^\circ \le L^\circ$, $j^K = \pm 1$. The K°-symmetrized basis set in eq 22 consists of eigenfunctions of the $C_2(y)$ operator which perform a π rotation about the y axis of the MF.[27]

An M symmetrization is useful in the high-field approximation, and for motions that are not extremely fast, so we can ignore the nonsecular terms in the spin Hamiltonian. However, in the presence of coupling to the cage a generalization of the standard M symmetrization is called for.[5,6,11,27] We may call it M_T symmetrization where $M_T = M^\circ + M^c$. In this case we have

$$|p^S q^S p^I q^I; L^\circ M^\circ K^\circ j^K L^c M^c j\rangle\rangle_M = \mathscr{N}^M[|p^S q^S p^I q^I; L^\circ M^\circ K^\circ j^K L^c M^c\rangle\rangle + js|p^S - q^S - p^I q^I; L^\circ - M^\circ K^\circ j^K L^c - M^c\rangle\rangle] \quad (25)$$

where

$$s = (-)^{L^\circ + L^c + M^\circ + M^c + q^S} \quad (26)$$

$$\mathscr{N}^M = [2(1 + \delta_{M^\circ,0}\delta_{M^c,0}\delta_{p^I,0}\delta_{q^S,0})]^{-1/2} \quad (27)$$

Equation 25 also requires that one constrains the quantum numbers p^I, M^c, M°, and q^S to the following five sets with corresponding values of j:

$$\left.\begin{array}{ll} (i) & p^I = 0, M^c = 0, M^\circ = 0, q^S = 0, j = (-)^{L^\circ + L^c} \\ (ii) & 0 < p^I \le 2I, M^c = 0, M^\circ = 0, q^S = 0, j = \pm 1 \\ (iii) & -2I \le p^I \le 2I, 0 < M^c \le L^c, M^\circ = 0, q^S = 0, j = \pm 1 \\ (iv) & -2I \le p^I \le 2I, -L^c \le M^c \le L^c, 0 < M^\circ \le L^\circ, q^S = 0, j = \pm 1 \\ (v) & -2I \le p^I \le 2I, -L^c \le M^c \le L^c, -L^\circ \le M^\circ \le L^\circ, q^S = 1, j = \pm 1 \end{array}\right\} \quad (28)$$

Note that if $q^S = 0$, then M° must be non-negative; also M^c is non-negative only if both $M^\circ = 0$ and $q^S = 0$.

We have combined both the K° and M_T symmetrizations to produce the fully symmetrized $|\Sigma\rangle\rangle_{KM}$ set. We shall find it useful to utilize a shorthand notation that will be extensively used in the calculation of matrix elements. It is implicitly defined by the following expression:

$$|\Sigma\rangle\rangle_{KM} = \mathscr{N}(|++\rangle\rangle + j^K s^K|+-\rangle\rangle + js|-+\rangle\rangle + j^K s^K js|--\rangle\rangle) \quad (29)$$

In eq 29 $|++\rangle\rangle$ refers to the uncoupled basis vector (eq 16)

which is specified by the same quantum numbers as that of $|\mathbf{\Sigma}\rangle\rangle_{KM}$, i.e.

$$|++\rangle\rangle = |L^{\circ}M^{\circ}K^{\circ}L^{c}M^{c}p^{S}q^{S}p^{I}q^{I}\rangle\rangle \tag{30}$$

Then $|+-\rangle\rangle$ is the uncoupled basis vector (UBV), in which K° has been replaced by $-K^{\circ}$. Similarly $|-+\rangle\rangle$ is the UBV where the set M°, M^{c}, p^{I}, and q^{S} is replaced by $-M^{\circ}$, $-M^{c}$, $-p^{I}$ and $-q^{S}$; and $|--\rangle\rangle$ is the UBV which has the set K°, M°, M^{c}, p^{I}, and q^{S} replaced by $-K^{\circ}$, $-M^{\circ}$, $-M^{c}$, $-p^{I}$, and $-q^{S}$.

4.2. Matrix and Vector Elements. Let us first proceed to evaluate the matrix elements of the stochastic Liouville operator in the unsymmetrized basis set. We shall then discuss the symmetry properties and the implementation of the symmetrized basis set. We shall consider matrix elements of the symmetrized stochastic Liouville operator which is related to the unsymmetrized form of eq 5 by

$$\tilde{\mathscr{L}} = P_{\mathrm{eq}}{}^{-1/2}\hat{\mathscr{L}}P_{\mathrm{eq}}{}^{1/2} = \tilde{\Gamma} + i\hat{\mathscr{H}}^{x} \tag{31}$$

where $\tilde{\Gamma} = P_{\mathrm{eq}}{}^{-1/2}\hat{\Gamma}P_{\mathrm{eq}}{}^{1/2}$.

The general matrix element of the spin Liouvillian in the unsymmetrized basis set is readily evaluated using eq 6:

$$\langle\langle\mathbf{\Sigma}_1|\hat{\mathscr{H}}^{x}|\mathbf{\Sigma}_2\rangle\rangle = \delta_{L_1^{c},L_2^{c}}\delta_{M_1^{c},M_2^{c}}[L_1^{\circ}L_2^{\circ}]^{1/2}(-)^{M_2^{c}+K_2^{\circ}} \times$$

$$\sum_{\mu=g,A}\sum_{l=0,2}\sum_{m=-l}^{l}\sum_{m'=-l}^{l}\sum_{m''=-l}^{l}\mathscr{D}^{l}_{mm'}(\Omega_d) \times$$

$$\begin{pmatrix} L_1^{\circ} & l & L_2^{\circ} \\ M_1^{\circ} & M_2^{\circ}-M_1^{\circ} & -M_2^{\circ}\end{pmatrix} \times$$

$$\begin{pmatrix} L_1^{\circ} & l & L_2^{\circ} \\ K_1^{\circ} & K_2^{\circ}-K_1^{\circ} & -K_2^{\circ}\end{pmatrix} F^{(l,m'')*}_{\mu,M}\langle\langle\boldsymbol{\sigma}_1|\hat{A}^{(l,m)}_{\mu,L}|\boldsymbol{\sigma}_2\rangle\rangle \tag{32}$$

where the effect of the spin operators is concentrated in the last factor, which just contains the reduced matrix elements for the spin part of the basis set. For completeness, we list in Appendix A these reduced matrix elements.

The calculation of the matrix elements of the two-body diffusional operator is somewhat more complicated. For clarity, we shall write the diffusional operator after separating it into four distinct contributions:

$$\tilde{\Gamma} = \tilde{\Gamma}^{\mathrm{sym}} + \tilde{\Gamma}^{\mathrm{asym}} + F^{\mathrm{sym}} + F^{\mathrm{asym}} \tag{33}$$

The first two terms represent the diffusion of both bodies in an isotropic medium; thus, they do not depend upon the potential. The axially symmetric term is

$$\tilde{\Gamma}^{\mathrm{sym}} = R_{\perp}^{\circ}\hat{\mathbf{J}}^{\circ 2} + (R_{\parallel}^{\circ} - R_{\perp}^{\circ})\hat{J}_z^{\circ 2} + R^{c}\hat{\mathbf{J}}^{c2} \tag{34}$$

(recall the discussion above for the cage diffusion). The asymmetric term represents the deviation from axially symmetric diffusion of the probe and is given by

$$\tilde{\Gamma}^{\mathrm{asym}} = R_d^{\circ}(\hat{J}_x^{\circ 2} + \hat{J}_y^{\circ 2}) \tag{35}$$

where

$$R_{\perp}^{\circ} = (R_x^{\circ} + R_y^{\circ})/2 \tag{36}$$

$$R_{\parallel}^{\circ} = R_z^{\circ} \tag{37}$$

$$R_d^{\circ} = (R_x^{\circ} - R_y^{\circ})/4 \tag{38}$$

The functions F^{sym} and F^{asym} depend upon the potential. They may be expressed in terms of the potential $v(\mathbf{\Omega}^{\circ},\mathbf{\Omega}^{c}) \equiv V(\mathbf{\Omega}^{\circ},\mathbf{\Omega}^{c})/k_{\mathrm{B}}T$, as

$$F^{\mathrm{sym}} = \frac{1}{2}[R_{\perp}^{\circ}(\hat{\mathbf{J}}^{\circ 2}v) + (R_{\parallel}^{\circ} - R_{\perp}^{\circ})(\hat{J}_z^{\circ 2}v)] - \frac{1}{4}[R_{\perp}^{\circ}(\hat{J}_{+}^{\circ}v)(\hat{J}_{-}^{\circ}v) + R_{\parallel}^{\circ}(\hat{J}_z^{\circ}v)^2] + \frac{R^{c}}{2}(\hat{\mathbf{J}}^{c2}v) - \frac{R^{c}}{4}[(\hat{J}_{+}^{c}v)(\hat{J}_{-}^{c}v) + (\hat{J}_z^{c}v)^2] \tag{39}$$

$$F^{\mathrm{asym}} = R_d^{\circ}\left\{(\hat{J}_{+}^{\circ 2}v + \hat{J}_{-}^{\circ 2}v) - \frac{1}{2}[(\hat{J}_{+}^{\circ}v)^2 + (\hat{J}_{-}^{\circ}v)^2]\right\} \tag{40}$$

Note that $\hat{J}_{\pm}^{(\circ,c)} = \hat{J}_x^{(\circ,c)} \pm i\hat{J}_y^{(\circ,c)}$ are the raising and lowering operators for the probe and the cage:

$$\hat{J}_{\pm}^{\circ}|L^{\circ}M^{\circ}K^{\circ}\rangle = c^{\mp}_{L^{\circ}K^{\circ}}|L^{\circ}M^{\circ}K^{\circ} \mp 1\rangle \tag{41}$$

$$\hat{J}_{\pm}^{c}|L^{c}M^{c}K^{c}\rangle = c^{\mp}_{L^{c}K^{c}}|L^{c}M^{c}K^{c} \mp 1\rangle \tag{42}$$

where $c^{\pm}_{LK} = \sqrt{L(L+1) - K(K \pm 1)}$. Note the inverted action of the raising and lowering operators on the Wigner functions, due to the fact that the vector operators $\hat{\mathbf{J}}^{\circ}$ and $\hat{\mathbf{J}}^{c}$ are defined in moving frames. Let us now separate out the spin degrees of freedom, with respect to which the diffusional operator is obviously ineffective. Thus we shall write

$$\langle\langle\mathbf{\Sigma}_1|\tilde{\Gamma}|\mathbf{\Sigma}_2\rangle\rangle = \delta_{\sigma_1,\sigma_2}\langle\lambda_1|\tilde{\Gamma}|\lambda_2\rangle \tag{43}$$

where

$$|\lambda\rangle = |L^{\circ}M^{\circ}K^{\circ}L^{c}M^{c}\rangle \tag{44}$$

The matrix elements of $\tilde{\Gamma}^{\mathrm{sym}}$ and $\tilde{\Gamma}^{\mathrm{asym}}$ are readily evaluated as

$$\langle\lambda_1|\tilde{\Gamma}^{\mathrm{sym}}|\lambda_2\rangle = \delta_{\lambda_1,\lambda_2}[R_{\perp}^{\circ}L^{\circ}(L^{\circ}+1) + (R_{\parallel}^{\circ} - R_{\perp}^{\circ})K^{\circ 2} + R^{c}L^{c}(L^{c}+1)] \tag{45}$$

$$\langle\lambda_1|\tilde{\Gamma}^{\mathrm{asym}}|\lambda_2\rangle = \delta_{L_1^{\circ},L_2^{\circ}}\delta_{M_1^{c},M_2^{c}}\delta_{L_1^{c},L_2^{c}}\delta_{M_1^{c},M_2^{c}}\frac{R_{\mathrm{d}}^{\circ}}{2} \times [c^{-}_{L_2^{\circ}K_2^{\circ}}c^{-}_{L_2^{\circ}K_2^{\circ}-1}\,\delta_{K_1^{\circ},K_2^{\circ}-2} + c^{+}_{L_2^{\circ}K_2^{\circ}}c^{+}_{L_2^{\circ}K_2^{\circ}+1}\,\delta_{K_1^{\circ},K_2^{\circ}+2}] \tag{46}$$

The matrix element of eqs 39 and 40 are more complicated. Let us first write the potential and the functions F^{sym} and F^{asym} in the form of an expansion in "probe−cage" normalized Wigner functions, $|\lambda\rangle$:

$$v(\mathbf{\Omega}^{\circ},\mathbf{\Omega}^{c}) = \sum_{\lambda} v_{\lambda}|\lambda\rangle \tag{47}$$

$$F^{\mathrm{sym}}(\mathbf{\Omega}^{\circ},\mathbf{\Omega}^{c}) = \sum_{\lambda} f_{\lambda}^{\mathrm{sym}}|\lambda\rangle \tag{48}$$

$$F^{\mathrm{asym}}(\mathbf{\Omega}^{\circ},\mathbf{\Omega}^{c}) = \sum_{\lambda} f_{\lambda}^{\mathrm{asym}}|\lambda\rangle \tag{49}$$

We now let $v_{\lambda} = v_{\lambda}^{\circ} + v_{\lambda}^{c} + v_{\lambda}^{\mathrm{int}}$. The mean field potential acting on the probe gives the coefficients

$$\{v_{\lambda}^{\circ}\} = -\frac{8\pi^2}{[L^{\circ}L^{c}]^{1/2}}a^{L^{\circ}}_{|K^{\circ}|} \tag{50}$$

where $L^{\circ} = 2$ or 4, $M^{\circ} = 0$, $K^{\circ} = 0$ or ± 2, $L^{c} = 0$, and $M^{c} = 0$; the potential acting on the cage gives similarly

$$\{v_{\lambda}^{c}\} = -\frac{8\pi^2}{[L^{\circ}L^{c}]^{1/2}}b_0^{L^{c}} \tag{51}$$

where $L^{\circ} = 0$, $M^{\circ} = 0$, $K^{\circ} = 0$, $L^{c} = 2$ or 4, and $M^{c} = 0$. In

order to obtain a useful expansion of $v^{int}(\Omega)$, we first expand the $\mathcal{D}^L_{MK}(\Omega)$ as[25,26]

$$\mathcal{D}^L_{MK}(\Omega) = \sum_{M'}(-)^{M+M'}\mathcal{D}^L_{-M'-M}(\Omega^c)\mathcal{D}^L_{M'K}(\Omega^\circ) \quad (52)$$

with the result (noting that $M = 0$ in eq 14)

$$v_\lambda = -(-)^{M^\circ}\frac{8\pi^2}{[L^\circ L^c]^{1/2}}c^{L^\circ}_{|K^\circ|} \quad (53)$$

$L^\circ = 2$ or 4, $M^\circ = -L^\circ$ to L°, $K^\circ = 0$ or ± 2, $L^c = L^\circ$, and $M^c = -M^\circ$. Once the relations for the expansion coefficients of F^{sym} and F^{asym} in terms of those in v are found, the matrix elements for the diffusional operator can be easily calculated in terms of sums of integrals of three Wigner functions. The explicit expressions are included in Appendix B.

We may now discuss the symmetry properties which lead to significant reduction of the dimension of the stochastic Liouville matrix. We first note that the diffusional operator exhibits K° symmetry; that is, a change of sign of the K° indices leaves the matrix elements unchanged except for a phase factor:

$$\hat{\mathcal{T}}_K\langle\langle\Sigma_1|\tilde{\Gamma}|\Sigma_2\rangle\rangle = (-)^{L_1^c+K_1^c+L_2^c+K_2^c}\langle\langle\Sigma_1|\tilde{\Gamma}|\Sigma_2\rangle\rangle \quad (54)$$

It also exhibits M_T symmetrization; that is, it is unaffected by a change of sign of the M°, M^c, p^I, and q^S indices simultaneously:

$$\hat{\mathcal{T}}_{M_T}\langle\langle\Sigma_1|\tilde{\Gamma}|\Sigma_2\rangle\rangle = (-)^{L_1^c+M_1^c+L_1^\circ+M_1^\circ+L_2^c+M_2^c+L_2^\circ+M_2^\circ}\langle\langle\Sigma_1|\tilde{\Gamma}|\Sigma_2\rangle\rangle \quad (55)$$

where we use $\hat{\mathcal{T}}_K$, $\hat{\mathcal{T}}_{M_T}$ to represent the operators for the two transformations.

The symmetry properties of the Liouville operator are less general. They are detailed by Meirovitch et al.[11] Here we only consider the properties of interest for the present case. If the g and A tensors have the same principal axis and the molecular tilt (i.e. the relative orientation of these tensors with respect to the MF) is defined by only a polar β angle,

$$\Omega_g = \Omega_A = (0,\beta,0) \quad (56)$$

then the K° symmetrization holds:

$$\hat{\mathcal{T}}_K\langle\langle\Sigma_1|\hat{\mathcal{H}}^x|\Sigma_2\rangle\rangle = (-)^{L_1^c+K_1^c+L_2^c+K_2^c}\langle\langle\Sigma_1|\hat{\mathcal{H}}^x|\Sigma_2\rangle\rangle \quad (57)$$

The M_T symmetrization does not hold, in general, for the Liouville operator. However, let us define the high-field limit by the following three conditions: (i) the applied microwave frequency of the experimental observation is close to the Larmor frequency, such that $|\omega - \omega_0| \ll \omega_0$; (ii) the magnetic field is much larger than the diagonal elements of the A tensor, $|A_{ii}| \ll B_0$; (iii) the difference between each of the principal values of the g tensor and g_0 is small, $|g_{ii} - g_0| \ll g_0$. In the high-field limit, for motions which are not too fast, the nonsecular terms in the spin Hamiltonian can be neglected. As a result, the three subspaces identified by $p^S = \pm 1$, $q^S = 0$ (*off-diagonal* subspaces) and $p^S = 0$, $q^S = \pm 1$ (*diagonal* subspace) are decoupled. In the following we shall consider only CW (one-dimensional) ESR experimental observations, which involve only the analysis of the off-diagonal subspace, since it is the only subspace coupled to the starting vector (see below). In this limit the M_T approximation holds:

$$\hat{\mathcal{T}}_{M_T}\langle\langle\Sigma_1|\hat{\mathcal{H}}^{xHF}|\Sigma_2\rangle\rangle = (-)^{L_1^c+M_1^c+L_1^\circ+M_1^\circ+L_2^c+M_2^c+L_2^\circ+M_2^\circ}\langle\langle\Sigma_1|\hat{\mathcal{H}}^{xHF}|\Sigma_2\rangle\rangle \quad (58)$$

Thus, in the high-field limit plus the constraint of only polar magnetic tilt, one may use eqs 54, 55, 57, and 58 and the definitions of the symmetrized basis sets, eqs 22 and 25, to show easily that the stochastic Liouville operator of eq 31 is block diagonal with respect to j^K and j. That is,

$$\langle\langle\Sigma_1|\tilde{\mathcal{L}}^{HF}|\Sigma_2\rangle\rangle_{KM} = \mathcal{N}_1\mathcal{N}_2(1 + j_1^K j_2^K)(1 + j_1 j_2)[\langle\langle{+}{+}|\tilde{\mathcal{L}}^{HF}|{+}{+}\rangle\rangle + j_2^K s_2^K\langle\langle{+}{+}|\tilde{\mathcal{L}}^{HF}|{+}{-}\rangle\rangle + j_2 s_2\langle\langle{+}{+}|\tilde{\mathcal{L}}^{HF}|{-}{+}\rangle\rangle + j_2^K s_2^K j_2 s_2\langle\langle{+}{+}|\tilde{\mathcal{L}}^{HF}|{-}{-}\rangle\rangle] \quad (59)$$

The factors $(1 + j_1^K j_2^K)$ and $(1 + j_1 j_2)$ guarantee that only elements of the M_T-symmetrized basis set diagonal with respect to j^K and j are nonzero in eq 59.

The CW-EPR spectrum relates to the x component in the LF of the electron spin magnetization, so that the appropriate starting vector is proportional to $\hat{S}_+$,[6]

$$|v_+\rangle\rangle = [I]^{-1/2}|\hat{S}_+ \otimes \mathbf{1}_I \otimes P_{eq}^{1/2}\rangle\rangle \quad (60)$$

where $\mathbf{1}_I$ is the unit operator in nuclear spin space. The elements of the starting vector in the symmetrized basis set are then given by

$$\langle\langle\Sigma|v_+\rangle\rangle_{KM} = \mathcal{N}\delta_{p^I,0}\delta_{|p^S|,1}(1 + j^K)(1 + j)\langle\lambda|P_{eq}^{1/2}\rangle \quad (61)$$

The reduced vector element $p_\lambda \equiv \langle\lambda|P_{eq}^{1/2}\rangle$ can be evaluated by factoring the equilibrium distribution and then using the completeness of the space spanned by the λ. We choose the following factorization:

$$P_{eq}(\Omega^\circ,\Omega^c) = \frac{Z^\circ Z^c}{Z}P^c(\Omega^c,\Omega^\circ)P^\circ(\Omega^\circ) \quad (62)$$

where $P^c(\Omega^c,\Omega^\circ)$ is the Boltzmann distribution with respect to $V^c(\Omega^c) + V^{int}(\Omega^\circ - \Omega^c)$ (cage effect), and $P^\circ(\Omega^\circ)$ is the Boltzmann distribution with respect to $V^\circ(\Omega^\circ)$ (probe mean field); Z, Z°, and Z^c are the overall, probe mean field, and cage effect partition functions, respectively. Each factored distribution can be projected onto the $|\lambda\rangle$ space:

$$P^c(\Omega^c,\Omega^\circ)^{1/2} = \sum_{\lambda'}p^c_{\lambda'}\lambda' \quad (63)$$

$$P^\circ(\Omega^\circ)^{1/2} = \sum_{\lambda''}p^\circ_{\lambda''}\lambda'' \quad (64)$$

so that

$$p_\lambda = \sqrt{\frac{Z^\circ Z^c}{Z}}\sum_{\lambda'}\sum_{\lambda''}p^\circ_{\lambda'}p^c_{\lambda''}\langle\lambda|\lambda'|\lambda''\rangle \quad (65)$$

The coefficients p^c_λ can be obtained after some algebraic manipulations in terms of simple integrals and sums of simple integrals:

$$p^c_\lambda = \langle\lambda|P^{c1/2}\rangle = \frac{1}{\sqrt{Z^c}}\frac{[L^\circ L^c]^{1/2}}{8\pi^2}\mathcal{P}(L^\circ L^c K^\circ)\delta_{M^\circ,-M^c} \times q^{int}_{L^\circ K^\circ}\sum_L [L]q^c_L\begin{pmatrix}L^\circ & L & L^c\\ -M^\circ & 0 & M^\circ\end{pmatrix}\begin{pmatrix}L^\circ & L & L^c\\ 0 & 0 & 0\end{pmatrix} \quad (66)$$

where $\mathcal{P}(n_1,n_2,...)$ is 0 if any one of the arguments is odd and

is unity otherwise. The integrals q_L^c and $q_{L^\circ K^\circ}^{int}$ depend respectively upon $\nu^c(\Omega^c)$ and $\nu(\Omega^\circ - \Omega^c)$:

$$q_L^c = \int_{-1}^{1} dz P_L^0(z) \exp[B(z)] \quad (67)$$

$$q_{L^\circ K^\circ}^{int} = 2\pi(2 - \delta_{K^\circ,0})\left[\frac{(L^\circ - K^\circ)!}{(L^\circ + K^\circ)!}\right]^{1/2} \times \int_{-1}^{1} dz P_{L^\circ}^{K^\circ}(z) \exp[C_1(z)] I_{K^\circ/2}[C_2(z)] \quad (68)$$

$$B(z) = \frac{1}{2} b_0^2 P_2^0(z) + \frac{1}{2} b_0^4 P_4^0(z) \quad (69)$$

$$C_1(z) = \frac{1}{2} c_0^2 P_2^0 + \frac{1}{2} c_0^4 P_4^0(z) \quad (70)$$

$$C_2(z) = \frac{1}{2\sqrt{6}} c_2^2 P_2^2(z) + \frac{1}{6\sqrt{10}} c_2^4 P_4^2(z) \quad (71)$$

where $P_l^m(\cos\beta)$ is the associate Legendre function of rank l and order m, and I_n is the modified Bessel function of rank n.[6] Similarly, the coefficients p_λ° may be reduced to a simple form. Indeed, they are just the coefficients of the expansion of the Boltzmann distribution of the system in the absence of the cage:

$$p_\lambda^\circ = \langle \lambda | P^{\circ 1/2} \rangle = \delta_{L^c,0}\delta_{M^c,0}\frac{1}{\sqrt{Z^\circ}}\sqrt{\frac{[L^\circ]}{8\pi^2}}\mathscr{D}(L^\circ K^\circ) q_{L^\circ K^\circ}^\circ \quad (72)$$

$$q_{L^\circ K^\circ}^\circ = 2\pi(2 - \delta_{K^\circ,0})\left[\frac{(L^\circ - K^\circ)!}{(L^\circ + K^\circ)!}\right]^{1/2} \times \int_{-1}^{1} dz P_{L^\circ}^{K^\circ}(z) \exp[A_1(z)] I_{K^\circ/2}[A_2(z)] \quad (73)$$

$$A_1(z) = \frac{1}{2} a_0^2 P_2^0(z) + \frac{1}{2} a_0^4 P_4^0(z) \quad (74)$$

$$A_2(z) = \frac{1}{2\sqrt{6}} a_2^2 P_2^2(z) + \frac{1}{6\sqrt{10}} a_2^4 P_4^2(z) \quad (75)$$

Note that the starting vector involves only basis functions with L^c even, and $j^K = j = 1$. Thus, since the stochastic Liouville operator is block diagonal with respect to j^K and j (cf. eq 59), only symmetrized basis vectors with $j^K = j = 1$ need to be retained. If the DF coincides with the LF (zero director tilt), an additional constraint can be imposed, such that both the stochastic Liouville matrix and the starting vector contain only symmetrized basis vectors for which $p^l = M^\circ + M^c$. This latter constraint also applies to isotropic fluids.

4.3. Computational Algorithms. The stochastic Liouville matrix constructed by the above procedure is a complex symmetric, but not Hermitian, matrix that is diagonalized by a complex orthogonal transformation.[6,11] Given the large number (eight) of degrees of freedom in the present case, one can generate matrices of dimension 10^4–10^5 even with the symmetry-based constraints that we have discussed above. Even though these matrices are very sparse, their computation is quite time consuming even by the Lanczos and related algorithms, which are known to be very efficient for such cases. Thus, we must first be careful to select the minimum basis $|\Sigma\rangle\rangle_{KM}$ that represents the spectrum without distortion. Thus, we first determined this minimum basis set by a general and objective method due to Vasavada et al. and referred to as the field-swept conjugate gradient method.[21,6] This method of "pruning" the basis set typically leads to order-of-magnitude reductions in its size from a nominally selected basis set. In applying this method we found a 3% pruning tolerance to be satisfactory for the present applications (that is, only basis vectors which have a projection greater than 0.03 onto the normalized starting vector for at least one magnetic field position within the spectrum are retained). For this minimum basis set one has a particular L_{max}° and L_{max}^c, which have been referred to above, but in addition, there are many combinations of the quantum numbers for which the respective basis vectors may be pruned out.

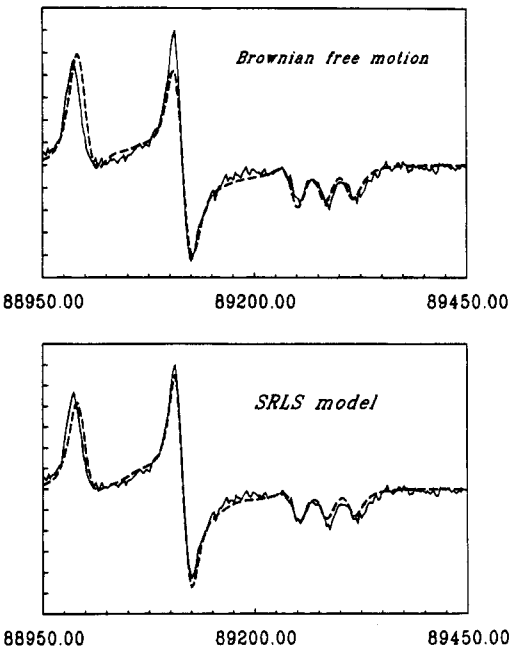

Figure 2. 250 GHz ESR spectrum of PDT in toluene obtained at −128 °C (solid line) compared to simulated best fit spectra (dashed lines) for models of (a, top) free Brownian reorientation and (b, bottom) the SRLS cage model.

Once the minimum basis set is obtained, then one may perform nonlinear least squares fitting of the simulated spectra to the experimental ones. Using the Marquardt–Levenberg procedure,[28–30] this usually involved 100–200 simulations to iterate to the best fitting parameters. For each simulation a variant of the Lanczos algorithm based upon conjugate gradients was used to tridiagonalize the stochastic Liouville matrix, followed by computing the spectrum by a continued fraction expansion.[6,19–21,27]

5. Comparison with Experiments

(a) PDT in Toluene. In the recent slow motional 250 GHz ESR study of PDT in toluene, it was found that the line shapes could not be satisfactorily fit by a simple Brownian model for the reorientation.[4] Instead, some jump types of motion were utilized to improve the fit. These jump types of motion involve introducing a "model-dependent" parameter $B_L^{(\mu)} = [1 + L(L+1)]^{-\mu}$ into the eigenvalues for simple rotational diffusion, e.g. $B_L^{(\mu)}\bar{R}L(L+1)$ (cf. eq 45). A value of the exponent $\mu \approx 1/2$ led to reasonable but still imperfect fits. (Largely for historical reasons the case $\mu = 1/2$ is referred to as "free diffusion".) However, the best fits to this "free diffusion" model did not show the expected dependence on solvent viscosity and temperature (cf. below).

We chose a slow motional spectrum obtained at −128 °C for this system. We show in Figure 2a the best fit to this slow motional spectrum for a Brownian motion model. Note the significant deviations between this fit and the experimental result. In Figure 2b we show the best fit obtained using the SRLS model. Note the overall significant improvement in fit. Of particular relevance is a feature of the Brownian motion

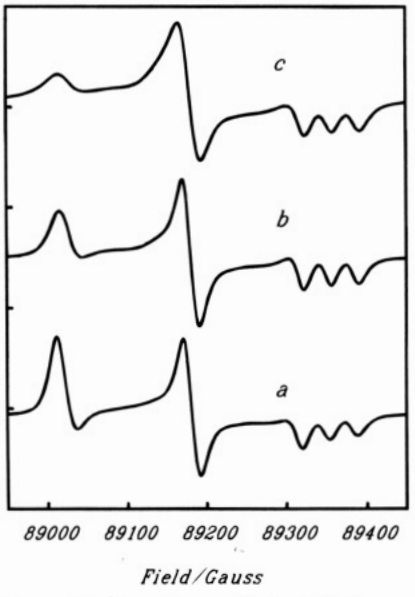

Figure 3. Effect of fourth-rank terms in the SRLS potential upon the predicted 250 GHz ESR spectrum of PDT in toluene: (a) free Brownian motion, i.e. no potential; (b) $c_0^4 = c_2^4 = 2k_BT$; (c) $c_0^4 = c_2^4 = 4k_BT$.

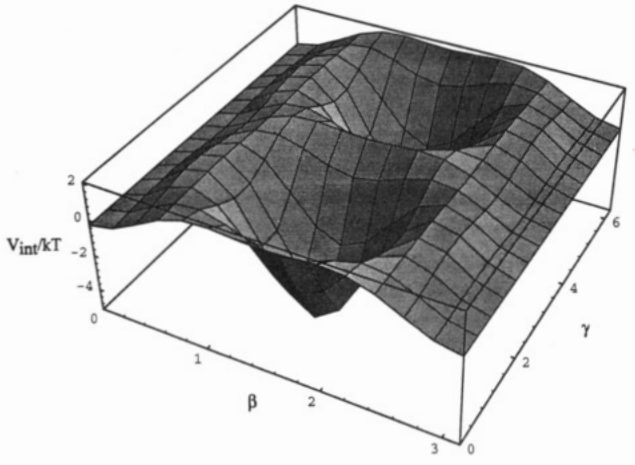

Figure 4. SRLS potential $v^{int}(\beta,\gamma)$ obtained from the best fit to the PDT in toluene spectrum, cf. Figure 2b. This figure corresponds to the following order parameters for PDT in the solvent cage: $\langle \mathscr{D}^2_{00} \rangle = -0.437$, $\langle \mathscr{D}^2_{02} \rangle = -0.482$, $\langle \mathscr{D}^4_{00} \rangle = 0.271$, $\langle \mathscr{D}^2_{00} \rangle = 0.253$.

simulations wherein there are sharp angular turns at the wings of the main spectral peaks. Such features do not exist in the experimental spectra, and they are indeed smoothed out in the SRLS simulation, thereby helping to provide an improved fit. We find that inclusion in eq 14 of terms in $\mathscr{D}^4_{0K}(\Omega)$ are more effective than terms in $\mathscr{D}^2_{0K}(\Omega)$ in providing this smoothing-out feature. We illustrate in Figure 3 the effect of the terms in $\mathscr{D}^4_{0K}(\Omega)$ in providing this smoothing out, although it should be noted that inclusion of terms in $\mathscr{D}^2_{0K}(\Omega)$ is also needed to provide the fit in Figure 2b. The effect of inclusion of terms of higher rank L will lead to more nodes in the potential (which go as $L + K$ for the spherical harmonics; recall $\mathscr{D}^L_{0K}(\Omega)^* \propto Y^L_K(\beta,\gamma)$). The actual potential $v^{int}(\Omega)$ given by eq 14 that was used in Figure 2b is illustrated in Figure 4. Note that there are two potential minima, both corresponding to the polar angle $\beta = \pi/2$ and with azimuthal angle $\gamma = \pi/2$ and $3\pi/2$. The potential barriers associated with these minima are close to $7k_BT$. Thus, the presence of this cage may be seen as modifying the Brownian reorientation to favor motion within regions near the potential minima and to have occasional jumps over the moderate potential barriers. In this sense we may regard the earlier simple jump models as limiting cases of jumping over potential barriers that are presumably more restrictive. [In this context we may speculate on the meaning of the exponent μ of the model parameter $B_L^{(\mu)}$ above. Values of $\mu = 0$ or 1 follow rigorously from simple Brownian vs jump diffusion (where the latter case is specialized for $\bar{R}\tau = 1$, with τ the mean time between jumps). A value of $0 < \mu < 1$ might be interpreted to imply a potential of the sort of Figure 4, which, we have noted, implies motion intermediate between Brownian diffusion and simple jump diffusion.] Clearly, by introducing terms of higher rank L and order K into the expansion of eq 14, it would be possible to produce more closely spaced potential minima, but in the present work we preferred to restrict this expansion to a set that could justifiably be fit to the experiment. Also, it is to be noted that by eq 14 we have imposed the uniaxial symmetry of the cage and the D_2 point group for the PDT.

For PDT the magnetic x axis is along the N−O bond and the magnetic z axis is along the nitrogen p-π orbital, with the magnetic y axis perpendicular to both. Figure 4 is associated with x ordering; that is, the magnetic x axis is taken as the principal axis of alignment and diffusion of the PDT with respect to the assumed uniaxial interaction potential due to the cage. Thus, the polar angle β refers to the alignment of this magnetic x axis in the cage, and the azimuthal angle γ refers to the relative alignment of the magnetic z and y axes. The minima in γ at $\pi/2$ and $3\pi/2$, with $\beta \approx \pi/2$, imply that alignment of the magnetic z axis with respect to the cage is favored, relative to alignment of the magnetic y axis when β is tilted toward $\pi/2$. Alignment of the magnetic z axis in order to get overlap of the N−O π orbital with the π orbitals of the toluene rings is, of course, to be expected.

The best fit parameters that we obtain for the SRLS model shown in Figure 2b are $\bar{R}^\circ = \sqrt[3]{R_x^\circ R_y^\circ R_z^\circ} = 8.91 \times 10^6\ s^{-1}$ and $N = R_x^\circ/\sqrt{R_z^\circ R_y^\circ} = 1.5$, with $R_z^\circ = R_y^\circ$ following Earle et al.,[4] since the motional spectra are insensitive to the ratio R_y°/R_z°. [This is nearly the same as the value of 1.6 used in ref 4. The result for N in that paper was given in the diffusion frame x, y, z, in which $x_M \rightarrow z$ and $z_M \rightarrow x$, but this was not clearly stated. We specify the magnetic frame x_M, y_M, z_M in the text but drop the subscript for convenience.] Also, $R^c = 7.94 \times 10^5\ s^{-1}$. The potential parameters giving rise to Figure 4 are $c_0^2 = -1.97$, $c_2^2 = -2.19$, $c_0^4 = 2.22$, and $c_2^4 = 1.10$. The best fit parameters for the free Brownian diffusion model shown in Figure 2a are $\bar{R}^\circ = 1.26 \times 10^7\ s^{-1}$ and $N = 1.3$, values that are rather close to those obtained from the SRLS model for these parameters. Note that R^c is just about 1 order of magnitude slower than $\bar{R}^\circ$, consistent with a persistent cage or local structure provided by the toluene solvent molecules around the PDT.

When one compares the present SRLS fit with that from the "free diffusion" model in ref 4, one can note some improvements in the fit. Of considerable potential interest is whether the present SRLS model will enable one to overcome some discrepancies found in previous ESR studies of PDT dynamics. Thus, in the work of ref 4 the graph of $\tau_{\bar{R}} \equiv 1/6\bar{R}^\circ$ vs η/T (η = solvent viscosity) shows the expected linear dependence for a Brownian model but not for the jump type of motion. It is possible that the SRLS model will not only produce good spectral simulations but will exhibit the expected η/T behavior for $\tau_{\bar{R}}$. This will require further study. A similar discrepancy was observed somewhat earlier between two-dimensional electron spin-echo results which favored Brownian motion vs CW-ESR results (both at 9.5 GHz)[31] which favored jump-type motions for PDT in 85% glycerol/15% water. Again, the SRLS model, which contains features of both Brownian motion and jump motion, might be useful to resolve such a discrepancy.

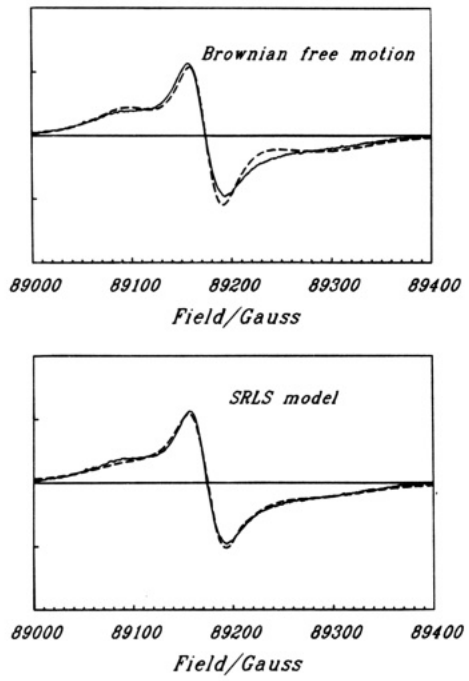

Figure 5. 250 GHz ESR spectrum of CSL in OTP obtained at 52 °C (solid line) compared to simulated best fit spectra (dashed lines) for models of (a, top) free Brownian reorientation and (b, bottom) the SRLS cage model.

(b) CSL in *o*-Terphenyl (OTP). The CSL spin-probe is larger than PDT and is cigar-shaped. It has recently been studied in toluene[4] and appeared to be fit by a mixed model of simple Brownian motion for its long axis with free diffusional motion about this axis. (The latter feature was introduced to make the rotational anisotropy N_y (cf. below) correspond to its value obtained from fast motional spectra.) For CSL, the magnetic z axis is parallel to the rotational y axis, and the magnetic y axis is tilted 15° with respect to the diffusional z axis, leading to a corresponding tilt between the magnetic x axis and the diffusional x axis. (Note that the magnetic axes for the nitroxide moiety of CSL are defined in an equivalent manner to PDT.) We have now carried out an extensive study of CSL in the glass-forming liquid OTP.[32] We show in Figure 5 one such spectrum taken at 52 °C. It is compared in Figure 5a with the best fit in the case of simple Brownian motion and in Figure 5b with the best fit SRLS model. Again we see how the SRLS model significantly improves the fit. The best fit parameters obtained for Figure 5b are $\bar{R}^\circ = 1.20 \times 10^8\ s^{-1}$, $N_y = R_y^\circ/\sqrt{R_x^\circ R_y^\circ} = 5.6$, and $R^c = 3.07 \times 10^6\ s^{-1}$ with $c_0^2 = -1.49$ and $c_2^2 = 0.74$. This is to be compared with the best fit values for simple Brownian motion of $\bar{R}^\circ = 0.89 \times 10^8\ s^{-1}$ and $N_y = 6.3$. Also, we note that for CSL in toluene a value of $N_y = 4.3$ was found from the fast motional spectrum. The cage diffusion is found to be somewhat more than 1 order of magnitude slower than that of the probe.

We show in Figure 6 the cage potential obtained in this case. Note that it is somewhat weaker than for PDT in toluene. More interesting is the fact that we obtain negative ordering for CSL in OTP. This may be rationalized simply. In OTP the planes of the phenyl groups are tilted with respect to each other. This enables a clathrate structure (or cage) in the OTP that has an oblate shape, which implies local discotic structure. The local director would then be perpendicular to the oblate structure. The cigar-like CSL would most naturally fit with its long axis perpendicular to the local director, corresponding to negative ordering.

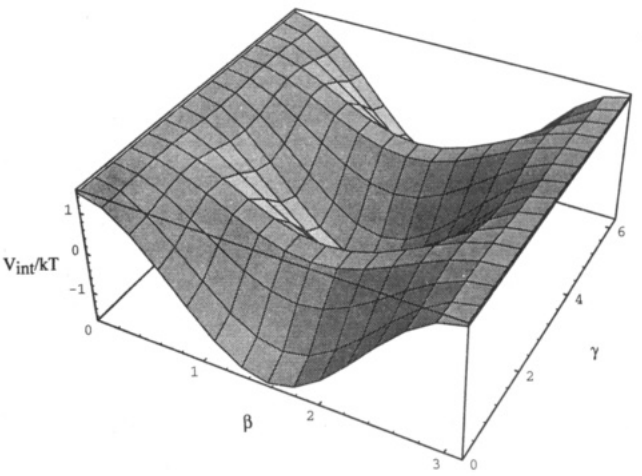

Figure 6. SRLS potential $v^{int}(\beta,\gamma)$ obtained from the best fit to the CSL in OTP spectrum, cf. Figure 5b. This figure corresponds to the following order parameters for CSL in the solvent cage: $\langle \mathscr{D}^2_{00} \rangle = -0.244$, $\langle \mathscr{D}^2_{02} \rangle = -0.187$.

We would also like to comment about the basis set size that is needed in these calculations (cf section 4.3). For the case of PDT in toluene at −128 °C convergence is achieved with $L^\circ_{max} = 14$, $M^\circ_{max} = K^\circ_{max} = 10$, and $L^c_{max} = M^c_{max} = 10$. With these maximum quantum numbers one has a basis set of dimension 13 956. However, after "pruning" (cf. section 4.3) the minimum basis set has dimension 2718 or a reduction by just over a factor of 5. Such a substantial reduction of dimension greatly speeds up the process of fitting, by nonlinear least squares, of the model to experiment. Another significant point is that $L^c_{max} < L^\circ_{max}$, although, as noted, $\bar{R}^\circ$ is more than 1 order of magnitude faster than R^c, and slower motions do require larger values of L_{max}.[5,6] This is explained by the fact that the cage orientation is a hidden variable; that is, it is not explicitly contained in the spin Hamiltonian of eq 1, although the probe orientation is explicitly contained when expanded out according to eq 6. The cage variables have an implicit or indirect effect on the ESR spectrum via the interaction potential of eq 11 that results in the coupled diffusion of probe + cage (of eq 9). Thus, less basis vectors are needed to represent the role of the cage variables on the ESR spectrum. In fact, given that an $M^\circ_{max} = 10$ was required, then the constraint of $p^l = M^\circ + M^c$ would imply an $M^c_{max} \approx M^\circ_{max}$ as found, in order to adequately represent the effect of the interaction potential. Then, of course, the smallest possible value of L^c_{max} is equal to M^c_{max}. Thus, additional or "hidden" degrees of freedom need not increase the dimension of the matrix representation of the augmented SLE as substantially as one might otherwise expect.

6. Summary

In this work we have developed an augmented SLE, which is designed to account for solvent cage effects on molecular reorientation in a variety of isotropic and ordered fluids by introducing a collective description of the cage in terms of a slowly relaxing local structure. The formal model is consistent with a recent molecular dynamics study of a simple fluid.[15] By careful consideration of the detailed structure of the matrix representation and its symmetries, it was possible to develop a relatively efficient computational formulation which allowed the simultaneous fitting by least squares methods of probe and cage variables to illustrative experiments. These cases yield a cage that relaxes slowly (at least 1 order of magnitude slower) than the probe reorientation, consistent with a fairly persistent cage, and that provides a potential only somewhat larger than k_BT

(on the order of 2−7 k_BT). In the context of a limited number of spherical harmonic terms in the interaction potential and of simplifying assumptions on the symmetry of this potential, some details of the form of this collective cage potential could be obtained. Thus, for PDT in toluene, potential minima at several reorientational angles in the cage were required for satisfactory fits, whereas for CSL in OTP a negative ordering of the CSL characteristic of an oblate-shaped cage structure was required. We regard this study as a demonstration of the considerable potential utility of analyzing slow motional ESR spectra to learn more about the dynamic structure of complex fluids. The model we employed is designed to replace the traditional but oversimplified reliance on jump-type models. Clearly the demonstration and confirmation of adequate models will require studies with a variety of probes and a range of solvents. We plan to report in the future on more extensive studies of several spin probes in OTP solvent over a range of temperatures by 250 GHz ESR[32] and studies of several spin-probes in liquid-crystal solvents by two-dimensional Fourier transform ESR,[33] a technique which has also been shown to be particularly sensitive to the molecular dynamics.[22,27]

Acknowledgment. The authors are indebted to Drs. D. E Budil, K. A. Earle, S. Lee, and R. H. Crepeau for useful discussions, and to D. J. Schneider for his enlightening suggestions. This work was supported by National Science Foundation Grants CHE93 13167 and DMR 9210638, by NIH Grants RR07126 and GM25862, by the Italian Ministry for Universities and Scientific and Technological Research, and in part by the National Research Council through its Centro Studi sugli Stati Molecolari. The computations reported here were performed at the Cornell Theory Center.

Appendix A: Spin Liouville Matrix Elements

We summarize here the components of the F and A tensors, in the notation of Meirovitch, Igner, Igner, Moro, and Freed.[11,6] The $F_{g,G}^{(l,m)}$ are given by

$$F_{g,G}^{(0,0)} = -\frac{1}{\sqrt{3}}\left(\frac{\beta_e}{\hbar}\right)(g_{xx} + g_{yy} + g_{zz}) \tag{76}$$

$$F_{g,G}^{(2,\pm2)} = \frac{1}{2}\left(\frac{\beta_e}{\hbar}\right)(g_{xx} - g_{yy}) \tag{77}$$

$$F_{g,G}^{(2,\pm1)} = 0 \tag{78}$$

$$F_{g,G}^{(2,0)} = \sqrt{\frac{2}{3}}\left(\frac{\beta_e}{\hbar}\right)\left[g_{zz} - \frac{1}{2}(g_{xx} + g_{yy})\right] \tag{79}$$

The components of the tensor product of $\mathbf{B}_0$ and $\hat{\mathbf{S}}$ are given in the LF by

$$A_{g,L}^{(0,0)} = -\frac{1}{\sqrt{3}}B_0\hat{S}_z \tag{80}$$

$$A_{g,L}^{(2,\pm2)} = 0 \tag{81}$$

$$A_{g,L}^{(2,\pm1)} = \mp\frac{1}{2}B_0\hat{S}_\pm \tag{82}$$

$$A_{g,L}^{(2,0)} = \sqrt{\frac{2}{3}}B_0\hat{S}_z \tag{83}$$

The hyperfine part of the Liouville operator is constructed in the same way. The F components are

$$F_{A,A}^{(0,0)} = -\frac{1}{\sqrt{3}}\left(\frac{g_e\beta_e}{\hbar}\right)(A_{xx} + A_{yy} + A_{zz}) \tag{84}$$

$$F_{A,A}^{(2,\pm2)} = \frac{1}{2}\left(\frac{g_e\beta_e}{\hbar}\right)(A_{xx} - A_{yy}) \tag{85}$$

$$F_{A,A}^{(2,\pm1)} = 0 \tag{86}$$

$$F_{A,A}^{(2,0)} = \sqrt{\frac{2}{3}}\left(\frac{g_e\beta_e}{\hbar}\right)\left[A_{zz} - \frac{1}{2}(A_{xx} + A_{yy})\right] \tag{87}$$

and the A components are

$$A_{A,L}^{(0,0)} = -\frac{1}{\sqrt{3}}\left[\hat{S}_z\hat{I}_z + \frac{1}{2}(\hat{S}_+\hat{I}_- + \hat{S}_-\hat{I}_+)\right] \tag{88}$$

$$A_{A,L}^{(2,\pm2)} = \frac{1}{2}\hat{S}_\pm\hat{I}_\pm \tag{89}$$

$$A_{A,L}^{(2,\pm1)} = \mp\frac{1}{2}(\hat{S}_\pm\hat{I}_z + \hat{S}_z\hat{I}_\pm) \tag{90}$$

$$A_{A,L}^{(2,0)} = \sqrt{\frac{2}{3}}\left[\hat{S}_z\hat{I}_z - \frac{1}{4}(\hat{S}_+\hat{I}_- + \hat{S}_-\hat{I}_+)\right] \tag{91}$$

The matrix elements in the spin subspace have also been reported by Meirovitch et al.[11] The A part is given by

$$\langle\langle\boldsymbol{\sigma}_1|\hat{A}_{A,L}^{(l,m)}|\boldsymbol{\sigma}_2\rangle\rangle = \delta_{m,\Delta p}\delta_{|\Delta p^S|,|\Delta q^S|}\delta_{|\Delta p^I|,|\Delta q^I|}\delta_{\Delta p^S\Delta p^I,\Delta q^S\Delta q^I} \times (-)^{\Delta p}[l]^{1/2}\begin{pmatrix}1 & 1 & l\\ \Delta p^S & \Delta p^I & -\Delta p\end{pmatrix}S_A \tag{92}$$

where $\Delta p(q)^i = p(q)_2^i - p(q)_1^i$ ($i = I, S$) and $\Delta p = \Delta p^S + \Delta p^I$; S_A is

$$\left.\begin{aligned}&\Delta p^S = 0,\ \Delta p^I = 0,\ S_A = (p_1^Sq_1^I + p_1^Iq_1^S)/2\\ &\Delta p^S = 0,\ \Delta p^I \neq 0,\ S_A = -(p_1^S\Delta p^I + q_1^S\Delta q^I)K_I/8\\ &\Delta p^S \neq 0,\ \Delta p^I = 0,\ S_A = -(p_1^I\Delta p^S + q_1^I\Delta q^S)/8\\ &\Delta p^S \neq 0,\ \Delta p^I \neq 0,\ S_A = \Delta p^S\Delta q^IK_I/2\end{aligned}\right\} \tag{93}$$

where $K_I = [I(I+1) - (q_1^I\Delta q^I + p_1^I\Delta p^I)(q_1^I\Delta q^I + p_1^I\Delta p^I - 2)/4]^{1/2}$. The g part is given by

$$\langle\langle\boldsymbol{\sigma}_1|\hat{A}_{g,L}^{(l,m)}|\boldsymbol{\sigma}_2\rangle\rangle = \delta_{m,\Delta p}\delta_{\Delta p^I,0}\delta_{\Delta q^I,0}\delta_{|\Delta p|,|\Delta q|}B_0 \times (-)^{\Delta p}[l]^{1/2}\begin{pmatrix}1 & 1 & l\\ \Delta p & 0 & -\Delta p\end{pmatrix}S_g \tag{94}$$

where S_g is

$$\left.\begin{aligned}&\Delta p^S = 0,\ S_g = p_1^S\\ &\Delta p^S \neq 0,\ S_g = -\Delta q^S/\sqrt{2}\end{aligned}\right\} \tag{95}$$

Appendix B: F Expansion of the Diffusional Operator

The expressions for F^{sym} and F^{asym} in terms of $|\lambda\rangle$ are obtained by expanding eqs 39 and 40, using eqs 47−49. The λth

coefficient for the symmetric part is found to be

$$f_\lambda^{\mathrm{sym}} = \frac{1}{2}[R_\perp^\circ L^\circ(L^\circ+1) + (R_\parallel^\circ - R_\perp^\circ)K^{\circ 2} + R_\perp^c L^c(L^c+1)]v_\lambda - \frac{1}{4}(-)^{M^\circ+K^\circ+M^c} \times \sum_{\lambda'\lambda''} \frac{[L^\circ L^{\circ\prime} L^{\circ\prime\prime} L^c L^{c\prime} L^{c\prime\prime}]^{1/2}}{8\pi^2} \times \delta_{M^\circ,M^{\circ\prime}+M^{\circ\prime\prime}}\delta_{K^\circ,K^{\circ\prime}+K^{\circ\prime\prime}}\delta_{M^c,M^{c\prime}+M^{c\prime\prime}}v_{\lambda'}v_{\lambda''} \times \begin{pmatrix} L^\circ & L^{\circ\prime} & L^{\circ\prime\prime} \\ -M^\circ & M^{\circ\prime} & M^{\circ\prime\prime} \end{pmatrix}\begin{pmatrix} L^c & L^{c\prime} & L^{c\prime\prime} \\ 0 & 0 & 0 \end{pmatrix} \times \left\{\begin{pmatrix} L^c & L^{c\prime} & L^{c\prime\prime} \\ -M^c & M^{c\prime} & M^{c\prime\prime} \end{pmatrix}\left[R_\parallel^\circ K^{\circ\prime}K^{\circ\prime\prime}\begin{pmatrix} L^\circ & L^{\circ\prime} & L^{\circ\prime\prime} \\ -K^\circ & K^{\circ\prime} & K^{\circ\prime\prime} \end{pmatrix} + R_\perp^\circ c^-_{L^{\circ\prime}K^{\circ\prime}}c^+_{L^{\circ\prime\prime}K^{\circ\prime\prime}}\begin{pmatrix} L^\circ & L^{\circ\prime} & L^{\circ\prime\prime} \\ -K^\circ & K^{\circ\prime}-1 & K^{\circ\prime\prime}+1 \end{pmatrix}\right] + R^c\begin{pmatrix} L^\circ & L^{\circ\prime} & L^{\circ\prime\prime} \\ -K^\circ & K^{\circ\prime} & K^{\circ\prime\prime} \end{pmatrix}\left[M^{c\prime}M^{c\prime\prime}\begin{pmatrix} L^c & L^{c\prime} & L^{c\prime\prime} \\ -M^c & M^{c\prime} & M^{c\prime\prime} \end{pmatrix} + c^+_{L^{c\prime}M^{c\prime}}c^-_{L^{c\prime\prime}M^{c\prime\prime}}\begin{pmatrix} L^c & L^{c\prime} & L^{c\prime\prime} \\ -M^c & M^{c\prime}-1 & M^{c\prime\prime}+1 \end{pmatrix}\right]\right\} \quad (96)$$

A similar expression holds for $f_\lambda^{\mathrm{asym}}$:

$$f_\lambda^{\mathrm{asym}} = \frac{R_d^\circ}{4}\left\{(c^-_{L^\circ K^\circ+2}c^-_{L^\circ K^\circ+1}v_{L^\circ M^\circ K^\circ+2L^c M^c} + c^+_{L^\circ K^\circ-2}c^+_{L^\circ K^\circ-1}v_{L^\circ M^\circ K^\circ-2L^c M^c}) + \sum_{\lambda'\lambda''}\frac{[L^\circ L^{\circ\prime} L^{\circ\prime\prime} L^c L^{c\prime} L^{c\prime\prime}]^{1/2}}{8\pi^2}\delta_{M^\circ,M^{\circ\prime}+M^{\circ\prime\prime}}\delta_{M^c,M^{c\prime}+M^{c\prime\prime}}v_{\lambda'}v_{\lambda''} \times \left[\delta_{K^\circ,K^{\circ\prime}+K^{\circ\prime\prime}-2}c^-_{L^{\circ\prime}K^{\circ\prime}}c^-_{L^{\circ\prime\prime}K^{\circ\prime\prime}}\begin{pmatrix} L^\circ & L^{\circ\prime} & L^{\circ\prime\prime} \\ -K^\circ & K^{\circ\prime}-1 & K^{\circ\prime\prime}-1 \end{pmatrix} + \delta_{K^\circ,K^{\circ\prime}+K^{\circ\prime\prime}+2}c^+_{L^{\circ\prime}K^{\circ\prime}}c^+_{L^{\circ\prime\prime}K^{\circ\prime\prime}}\begin{pmatrix} L^\circ & L^{\circ\prime} & L^{\circ\prime\prime} \\ -K^\circ & K^{\circ\prime}+1 & K^{\circ\prime\prime}+1 \end{pmatrix}\right] \times \begin{pmatrix} L^\circ & L^{\circ\prime} & L^{\circ\prime\prime} \\ -M^\circ & M^{\circ\prime} & M^{\circ\prime\prime} \end{pmatrix}\begin{pmatrix} L^c & L^{c\prime} & L^{c\prime\prime} \\ -M^c & M^{c\prime} & M^{c\prime\prime} \end{pmatrix}\begin{pmatrix} L^c & L^{c\prime} & L^{c\prime\prime} \\ 0 & 0 & 0 \end{pmatrix}\right\} \quad (97)$$

The matrix elements of F^{sym} and F^{asym} are then completely defined in terms of the integral of three $|\lambda\rangle$ functions, which is known from the properties of the Wigner functions:[25,26]

$$\langle\lambda_1|\lambda_2|\lambda_3\rangle = \sqrt{\frac{[L_1^\circ L_1^c L_2^\circ L_2^c L_3^\circ L_3^c]}{8\pi^2}}(-)^{M_1^\circ+M_1^c+K_1^\circ} \times \begin{pmatrix} L_1^\circ & L_2^\circ & L_3^\circ \\ M_1^\circ & -M_2^\circ & -M_3^\circ \end{pmatrix}\begin{pmatrix} L_1^\circ & L_2^\circ & L_3^\circ \\ K_1^\circ & -K_2^\circ & -K_3^\circ \end{pmatrix} \times \begin{pmatrix} L_1^c & L_2^c & L_3^c \\ M_1^c & -M_2^c & -M_3^c \end{pmatrix}\begin{pmatrix} L_1^c & L_2^c & L_3^c \\ 0 & 0 & 0 \end{pmatrix} \quad (98)$$

References and Notes

(1) Lebedev, Ya. S. In *Modern Pulsed and Continuous Wave Electron Spin Resonance*; Kevan, L., Bowman, M. K., Eds.; Wiley: New York, 1990; Chapter 8.

(2) Lyubashevskaya, E. V.; Antisiferova, L. I.; Lebedev, Ya. S. *Teor. Eksp. Kim.* **1987**, *23*, 46.

(3) Budil, D. E.; Earle, K. A.; Lynch, W. B.; Freed, J. H. *Advanced EPR: Applications in Biology and Biochemistry*; Hoff, A. J., Ed.; Elsevier: Amsterdam, 1989; Chapter 8.

(4) Earle, K. A.; Budil, D. E.; Freed, J. H. *J. Phys. Chem.* **1993**, *97*, 13289.

(5) Freed, J. H. In *Spin Labeling: Theory and Applications*; Berliner, L., Ed.; Academic Press: New York, 1976; p 53.

(6) Schneider, D. J.; Freed, J. H. (a) *Adv. Chem. Phys.* **1989**, *73*, 387; (b) *Biological Magnetic Resonance*; Berliner, L. J., Reuben, J., Eds.; Plenum: New York, 1989; Vol. 8, p 1.

(7) Hwang, J. S.; Mason, R. P.; Hwang, L.-P.; Freed, J. H. *J. Phys. Chem.* **1975**, *79*, 489.

(8) Zager, S. A.; Freed, J. H. *J. Chem. Phys.* **1982**, *77*, (a) 3344, (b) 3360.

(9) Polnaszek, C. F.; Freed, J. H. *J. Phys. Chem.* **1975**, *79*, 2283.

(10) Campbell, R. F.; Freed, J. H. *J. Phys. Chem.* **1980**, *84*, 2668.

(11) Meirovitch, E.; Igner, D.; Igner, E.; Moro, G.; Freed, J. H. *J. Chem. Phys.* **1982**, *77*, 3915.

(12) Freed, J. H. In *Rotational Dynamics of Small and Macromolecules*; Dörfmuller, T. F., Pecora, R., Eds.; Lecture Notes in Physics 293; Springer: Berlin, 1987; p 89.

(13) Polimeno, A.; Freed, J. H. *Chem. Phys. Lett.* **1990**, *174*, (a) 338, (b) 481.

(14) Polimeno, A.; Freed, J. H. *Adv. Chem. Phys.* **1993**, *83*, 89.

(15) Polimeno, A.; Moro, G. J.; Freed, J. H. *J. Chem. Phys.* **1995**, *102*, 8094 and to be published.

(16) Freed, J. H. *J. Chem. Phys.* **1977**, *66*, 4183.

(17) Stillman, A. E.; Freed, J. H. *J. Chem. Phys.* **1980**, *72*, 550.

(18) Kivelson, D. In *Rotational Dynamics of Small and Macromolecules*; Dörfmuller, T. F., Pecora, R., Eds.; Lecture Notes in Physics 293; Springer: Berlin, 1987; p 1.

(19) Moro, G.; Freed, J. H. *J. Chem. Phys.* **1981**, *74*, 3757.

(20) Moro, G.; Freed, J. H. In *Large Scale Eigenvalue Problems*; Cullum, J., Willoughby, R. A., Eds.; North-Holland: Amsterdam, 1986.

(21) Vasavada, K. V.; Schneider, D. S.; Freed, J. H. *J. Chem. Phys.* **1987**, *86*, 647.

(22) Gorcester, J.; Rananavare, S.; Freed, J. H. *J. Chem. Phys.* **1989**, *90*, 5764.

(23) Moro, G.; Nordio, P. L. *J. Phys. Chem.* **1985**, *89*, 997.

(24) Freed, J. H.; Nayeem, A.; Rananavare, S. In *The Molecular Dynamics of Liquid Crystals*; Luckhurst, G. R., Veracini, C. A., Eds.; Kluwer: The Netherlands, 1994; p 71.

(25) Biedenharn, L. C.; Louck, J. D. *Angular Momentum*; Addison-Wesley: Reading, MA, 1981; Part I.

(26) Rose, M. E. *Elementary Theory of Angular Momentum*; Wiley: New York, 1957.

(27) Lee, S.; Budil, D. E.; Freed, J. H. *J. Chem. Phys.* **1994**, *101*, 5529.

(28) Crepeau, R. H.; Rananavare, S. B.; Freed, J. H. In *10th International EPR Symposium*; Rocky Mountain Conference, Denver, 1987.

(29) Shin, Y. K.; Freed, J. H. *Biophys. J.* **1989**, *55*, 537.

(30) Budil, D. E.; Lee, S.; Freed, J. H. To be published.

(31) Millhauser, G. L.; Freed, J. H. *J. Chem. Phys.* **1984**, *81*, 37; **1986**, *85*, 63.

(32) Earle, K. A.; Polimeno, A.; Moscicki, J.; Freed, J. H. To be published.

(33) Sastry, V. S. S.; Polimeno, A.; Crepeau, R. H.; Freed, J. H. To be published.

(34) Liang, Z.; Westlund, P. O.; Wikander, G. *J. Chem. Phys.* **1993**, *99*, 7098.

JP9504783